Materials Science and Engineering B 176 (2011) 1378–1381

Contents lists available at ScienceDirect

Materials Science and Engineering B

journal homepage: www.elsevier.com/locate/mseb

Magnetic and electronic properties of $Sn_{1-x}Cr_xO_2$ diluted alloys

Pablo D. Borges[a], Lui'sa M.R. Scolfaro[b,*], Horácio W. Leite Alves[c], Eronides F. da Silva Jr.[d], Lucy V.C. Assali[a]

[a] Instituto de Física, Universidade de São Paulo, CP 66318, 05315-970 São Paulo, SP, Brazil
[b] Department of Physics, Texas State University, San Marcos 78666, TX, USA
[c] Universidade Federal de São João Del Rei, CP 110, 36301-160 São João Del Rei, MG, Brazil
[d] Departamento de Fisica, Universidade Federal de Pernambuco, 50670-901 Recife, PE, Brazil

ARTICLE INFO

Article history:
Received 1 October 2010
Received in revised form
11 December 2010
Accepted 10 January 2011
Available online 26 January 2011

Keywords:
Dilute magnetic semiconductor
Oxides
$SnCrO_2$
Magnetic properties
Spintronics
Tin dioxide
Ab initio calculations

ABSTRACT

We present the results of first-principles electronic structure calculations of $Sn_{0.96}Cr_{0.04}O_2$ alloys, simulating chromium in rutile tin dioxide as an impurity in a diluted magnetic semiconductor configuration. A magnetic bistability has been observed, with the occurrence of a low-spin state with magnetic moment $m = 0\mu_B$ in addition to the high-spin ground state with $m = 2\mu_B$. When an oxygen vacancy is included, as one of the nearest-neighbors to Cr impurity, a remarkable change is observed in the magnetic metastability. The energy barrier for the crossover from the low-spin to high-spin is lowered by 75%. These findings suggest that these materials may be used in applications which require different magnetized states.

1. Introduction

In recent years, dilute magnetic semiconductors (DMSs) have attracted great attention from both experimental and theoretical points of view due to their potential application in spintronic devices where both the charge and the spin of the particles play a role. A key requirement in realizing most devices based on spins is that the host material must be ferromagnetic (FM) above 300 K. In addition, it is necessary to have efficient spin polarized carriers. One approach to achieve the spin injection is obtained by doping oxides or semiconductor materials with magnetic impurities in a DMS configuration. These systems are good candidates to obtain half-metallic behavior materials, with spin polarized carriers at the Fermi level.

Tin dioxide (SnO_2), a transparent wide band gap semiconducting oxide, doped with transition metals (TMs), has been extensively investigated recently due to the resulting important magnetic properties [1–6]. In particular, FM behavior has been observed at room temperature in Cr-doped SnO_2 DMS systems [7–9], indicating the potential of such systems for spintronic applications. It has also been observed that the presence of oxygen vacancies appears to be required for producing ferromagnetism in DMS oxides, such as, e.g., in Co- and Fe-doped ZnO [10–13], in Co-doped TiO_2 [14,15], in Fe- and Co-doping in In_2O_3 [16,17] and in Co- and Cr-doped SnO_2 [7,18,19]. A theoretical model proposed by Coey et al. to interpret the ferromagnetism in these semiconducting oxides requires the existence of oxygen vacancies in close proximity to TM sites in order to maintain the charge neutrality [20]. For Cr-doped SnO_2 nanoparticles, the FM behavior is limited by a maximum doping concentration x_L which has a strong relation with structural changes revealed from X-ray diffraction measurements [7]. The presence of oxygen vacancies in these $Sn_{1-x}Cr_xO_2$ samples, in which the Cr concentrations x varies from 0 to 10% has been detected by electron paramagnetic resonance (EPR) experiments [19]. The literature contains many efforts aimed at the characterization and understanding of the mechanisms involved in the FM behavior observed in such systems. However, no theoretical models based on rigorous ab initio electronic structure calculations have been published that establish unambiguously the roles played by Cr and by Cr with an oxygen vacancy nearby in SnO_2 [21].

In this work, we study the magnetic metastability and electronic properties of $Sn_{1-x}Cr_xO_2$ DMS alloys, for $x = 0.04$, i.e., $Sn_{0.96}Cr_{0.04}O_2$ alloys, through ab initio electronic structure calculations performed within the spin density functional theory. We have chosen the concentration of $x = 0.04$ for the calculations since, it corresponds to a typical experimental value (in the range under which most of the

* Corresponding author. Tel.: +1 512 2458610.
E-mail addresses: ls61@txstate.edu, lscolfaro@txstate.edu (L.M.R. Scolfaro).

0921-5107/$ – see front matter © 2011 Elsevier B.V. All rights reserved.
doi:10.1016/j.mseb.2011.01.017

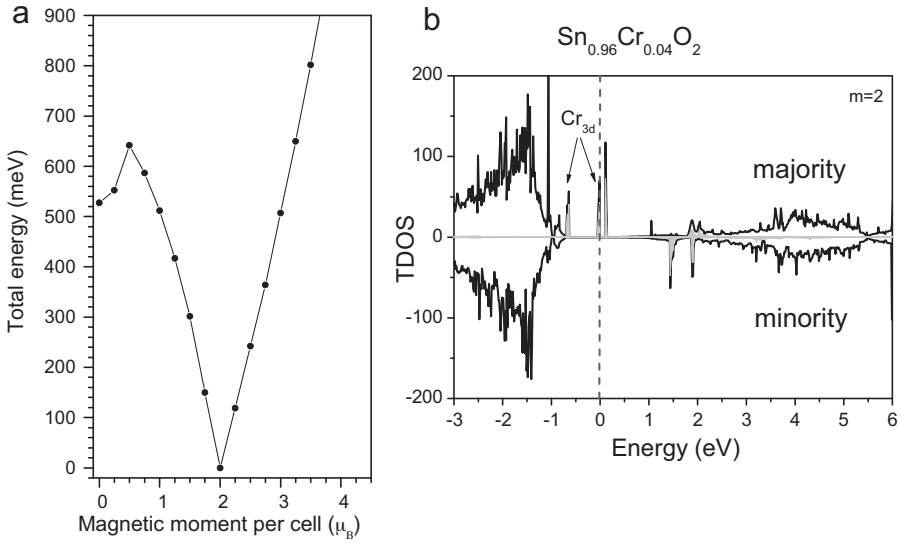

Fig. 1. (a) Total energy versus magnetic moment per cell. The total energy of the high spin ground state is set to zero; (b) the total (black lines) and projected (gray shaded areas) density of states of the Cr 3d derived states for the majority and minority spins for the magnetic moment equal to $2\mu_B$ are shown. The vertical (dashed) line placed at the energy zero corresponds to the highest occupied energy level for the majority spin.

experimental work has been done) and the alloy can be easily simulated by a reasonable size supercell. The magnetic metastability has been recently investigated in GaN:TM [22]. Importantly, we also study the influence of an oxygen vacancy nearest neighbor to the Cr atom in the alloys, $Sn_{1-x}Cr_xO_{2-y}(V_O)_y$ systems, with $x = 0.04$ and $y = 0.02$, i.e., $Sn_{0.96}Cr_{0.04}O_{0.98}(V_O)_{0.02}$ alloys, and its consequences SnO_2:Cr.

2. Calculation method

All calculations were based on the spin density functional theory. We employed the Projector Augmented Wave method implemented in the Vienna Ab initio Simulation Package (VASP–PAW) [23,24]. The exchange-correlation potential used was the generalized gradient approximation in the Perdew, Burke, and Ernzerhof (GGA–PBE) [25] approach. The method has been previously used to study the structural and electronic properties of bulk rutile SnO_2 [26]. The valence electronic distributions for the PAWs representing the atoms were Sn – $4d^{10}\ 5s^2\ 5p^2$, Cr – $3d^5\ 4s^1$, and O – $2s^2\ 2p^4$. Scalar relativistic effects were taken into account. To describe the alloys, we used a 72-atoms supercell (24 Sn and 48 O atoms) and a $4 \times 4 \times 4$ mesh of Monkhorst-Pack k-points for integration in the Brillouin zone. All the calculations were done with a 490 eV energy cut-off in the plane-wave expansions and the systems were fully relaxed until the residual forces on the ions were less than 10 meV/Å.

3. Results and discussion

Two DMS systems were studied, the $Sn_{0.96}Cr_{0.04}O_2$ and the $Sn_{0.96}Cr_{0.04}O_{1.98}(V_O)_{0.02}$ with the oxygen vacancy as the Cr nearest neighbor. For the system without the vacancy, a single Sn atom was substituted with a chromium atom in the 72-atoms supercell, simulating the $x = 0.04$ impurity concentration. For this configuration the calculation was performed at the D_2h symmetry. Fig. 1(a) shows the total energy versus the magnetic moment per cell for the $Sn_{0.96}Cr_{0.04}O_2$ alloy. We observe a high spin ground state with a magnetic moment $m = 2\mu_B$ and a low spin state with a magnetic moment $m = 0\mu_B$. For this case a spin crossover becomes possible with an energy barrier of 114 meV calculated for the transition from $m = 0\mu_B$ to $m = 2\mu_B$. We observe a relationship between the structural modification around the chromium atom, due to the electronic and ionic relaxations, and the appearance of the magnetic metastability. If we consider a spherical volume involving the chromium atom whose radius is an average distance between Cr and the six oxygen first-neighbors, our calculations showed that, after full relaxation the corresponding volume is reduced by about 16% for the high spin state ($2\mu_B$) and 17.5% for the low spin state ($0\mu_B$). These findings agree with our preliminary study of strain effects in bulk rutile CrO_2 which indicated a decrease in the magnetization when the volume was reduced, as well as with the experimental evidence that a decrease in the magnetic moment is followed by a volume reduction around Cr in $Sn_{1-x}Cr_xO_2$ alloys [19]. Our calculations showed that if the volume is reduced for more than 30% compared with the equilibrium bulk value in CrO_2, the system becomes non-magnetic. Similar results have been obtained by Srivastava et al. [27] in bulk CrO_2.

Moruzzi [28] has shown that the transition from non-magnetic to a magnetic behavior in the transition-metal ferromagnets can be understood by analyzing the volume dependence of the variation of the total energy with the magnetic moment. The presence or absence of magnetism in this case is determined by a competition between intra-atomic exchange interactions and inter-atomic electronic motion due to the crystalline field. This allows us to conclude that the observed magnetic metastability in the studied DMSs is because there is a structural modification (relaxation) around the chromium atom. The total and projected density of states (TDOS and PDOS, respectively) of chromium for the majority and minority spins for the magnetic moment $m = 2\mu_B$ is shown in Fig. 1(b). The vertical lines close to the energy zero represent the highest occupied energy levels for the majority spin. We observe that the chromium 3d derived orbital states appear in the gap region and show a half-metallic behavior.

Next we discuss results for $Sn_{0.96}Cr_{0.04}O_{1.98}(V_O)_{0.02}$ where an oxygen vacancy is one of the six first-neighbors of Cr. For the calculation of this complex pair we used a 72-atoms supercell in which a Cr atom replaces a Sn (one out of the 24 Sn atoms in the supercell) and one of the six oxygen nearest-neighbors is removed (out of the 48 O atoms in the supercell) leaving behind a vacancy. This system corresponds to an alloy with 4% and 2% concentrations of chromium and oxygen vacancy, respectively. For this configu-

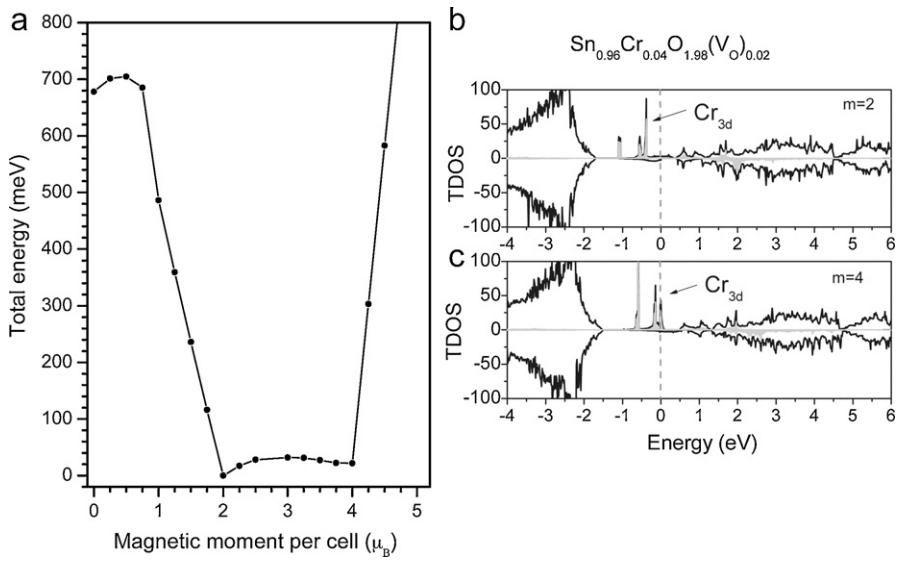

Fig. 2. (a) Total energy versus magnetic moment per cell. The total energy of the high spin ground state is set to zero. (b) Also shown are the total (black lines) and projected (gray shaded areas) density of states of the Cr 3d derived for the majority spin (upper panels) and the minority spin (lower panels) for the magnetic moment $m = 2\mu_B$ and $m = 4\mu_B$. The vertical (dashed) lines placed at the energy zero correspond to the highest occupied energy level for the majority spin.

ration the calculation was performed at C_{2v} symmetry. Fig. 2(a) shows the total energy versus the magnetic moment per cell for the $Sn_{.96}Cr_{.04}O_{1.98}(V_O)_{.02}$ alloys. We observe the appearance of a second high spin configuration, with magnetic moment $m = 4\mu_B$, and an almost flat region between $m = 2\mu_B$ and $m = 4\mu_B$. The ground state, however, remains as the $2\mu_B$ magnetic moment high-spin state. The energy barrier for the $m = 0\mu_B$ to $m = 2\mu_B$ transition was reduced to 27 meV. The same transition for the DMS without the vacancy was 114 meV, showing a drastic reduction by 75%. As discussed before, the magnetic configuration is determined by the volume dependence of the variation of the total energy with the magnetic moment. As previously, this can be evaluated by fixing a spherical volume around Cr such that inside this sphere radius there are five O atoms and the vacancy, and then comparing the obtained volumes for this sphere before and after the relaxations are performed. For the high spin states ($2\mu_B$ and $4\mu_B$) the volume reductions, after full relaxed calculations, were 20% and 22%, respectively, while for the low spin state ($0\mu_B$) it was 31%. The substantial lowering of the energy barrier can be understood by analyzing the volume reduction around chromium atom with and without an oxygen vacancy nearby. For $m = 2\mu_B$ the reductions are 20% and 16%, respectively, while for $m = 0\mu_B$ they are 31% and 17.5%, respectively. Therefore, for low-spin configurations the presence of a missing oxygen atom allows greater relaxations which reduce the total energy of the system lowering the energy barrier for the crossover.

The TDOS and PDOS of the Cr 3d orbital are shown in Fig. 2(b), for $m = 2\mu_B$ and $m = 4\mu_B$, respectively. The vertical lines at the energy zero represent the highest occupied energy values for the majority spin. As with the $SnCrO_2$ system, the chromium 3d states derived from the Cr plus an oxygen vacancy pair in SnO_2 are found to lie in the gap region and, for $m = 4\mu_B$ the system depicts a half-metallic behavior.

The crystal field theory can thus be used to understand the occurrence of magnetic metastability. The atomic *d*-level in the octahedral symmetry of the Sn site of the rutile structure splits into two levels (t_{2g} and e_g) when replaced by Cr, where the energy difference between these levels is called the crystal field splitting. Each level, t_{2g} and e_g, can still be split further due to intra-atomic exchange interactions. Therefore, the occurrence of the low-spin and high-spin states depends on the effective balance between these two interaction fields. The low-spin state occurs when the crystal field splitting is larger than the intra-atomic exchange splitting (lowest volume), otherwise, the high-spin state is the ground state (highest volume).

4. Conclusions

The magnetic and electronic properties of chromium as an impurity in a DMS configuration in rutile tin dioxide, ($Sn_{0.96}Cr_{0.04}O_2$), were studied using ab initio calculations performed within the spin-density functional theory. A magnetic metastability was observed, with the occurrence of a low-spin state with magnetic moment $m = 0\mu_B$ in addition to the high-spin ground state with $m = 2\mu_B$. An energy barrier of 114 meV was obtained for the spin crossover between the $m = 0\mu_B$ and $m = 2\mu_B$ states in $Sn_{0.96}Cr_{0.04}O_2$. When an oxygen vacancy is considered as one of the six first-neighbors to the Cr impurity in these alloys (the $Sn_{0.96}Cr_{0.04}O_{1.98}(V_O)_{0.02}$) a considerable modification is observed in the magnetic metastability behavior, with the occurrence of a second high-spin configuration with magnetic moment $m = 4\mu_B$, and with significantly lower energy barriers,~27 meV, for the system to flip from the low-spin to the high-spin state. This behavior is attributed to the relative contributions of the intra-atomic exchange interactions effect and the inter-atomic electron motion effect due to the crystalline field which are responsible for the relaxations around the chromium atom.

Acknowledgements

This work was partially supported by the Brazilian funding agencies FAPEMIG, FAPESP, CAPES, and CNPq, and by the Materials Science, Engineering and Commercialization Program at Texas State University in San Marcos. The authors also acknowledge Prof. T. H. Myers for the critical reading of the manuscript.

References

[1] Xavier Mathew, et al., J. Appl. Phys. 100 (2006), 073907.
[2] H. Kimura, et al., Appl. Phys. Lett. 80 (2002) 94.
[3] W. Wang, et al., J. Appl. Phys. 99 (2006), 08M115.
[4] S.B. Ogale, et al., Phys. Rev. Lett. 91 (2003) 077205.
[5] C.E. Rodrıguez Torres, J. Magn. Magn. Mater. 316 (2007) e219.

[6] Matthias Batzill, et al., Thin Solid Films 484 (2005) 132.
[7] C. Van Komen, A. Thurber, K.M. Reddy, J. Hays, A. Punnoose, J. Appl. Phys. 103 (2008), 07D141.
[8] N.H. Hong, J. Sakai, W. Prellier, A. Hassini, J. Phys.: Condens. Matter 17 (2005) 1697.
[9] C.B. Fitzgerald, et al., Phys. Rev. B 74 (2006) 115307.
[10] A. Fouchet, W. Prellier, P. Padhan, Ch. Simon, B. Mercey, V.N. Kulkarnib, T. Venkatesan, J. Appl. Phys. 95 (2004) 7187.
[11] B. Martínez, F. Sandiumenge, Ll. Balcells, J. Fontcuberta, F. Sibieude, C. Monty, J. Magn. Magn. Mater. 290–291 (2005) 168.
[12] R.K. Singhal, et al., J. Alloys Compd. 496 (2010) 324.
[13] A. Samariya, R.K. Singhal, S. Kumar, Y.T. Xing, M. Alzamora, S.N. Dolia, U.P. Deshpande, T. Shripathi, E. Saitovitch, Mater. Chem. Phys. 123 (2010) 678.
[14] R.K. Singhal, et al., Solid State Commun. 150 (2010), 1154.
[15] R.K. Singhal, et al., J. Appl. Phys. 107 (2010), 113916.
[16] A. Samariya, R.K. Singhal, S. Kumar, Y.T. Xing, S.C. Sharma, P. Kumari, D.C. Jain, S.N. Dolia, U.P. Deshpande, T. Shripathi, E. Saitovitch, Appl. Surf. Sci. 257 (2010) 585.
[17] R.K. Singhal, A. Samariya, S. Kumar, S.C. Sharma, Y.T. Xing, U.P. Deshpande, T. Shripathi, E. Saitovitch, Appl. Surf. Sci. 257 (2010) 1053.
[18] J. Hays, A. Punnoose, R. Baldner, M.H. Engelhard, J. Peloquin, K.M. Reddy, Phys. Rev. B 72 (2005), 075203.
[19] S.K. Misra, S.I. Andronenko, S. Rao, S.V. Bhat, Chadd Van Komen, A. Punnoose, J. Appl. Phys. 105 (2009), 07C514.
[20] J.M.D. Coey, et al., Nat. Mater. 4 (173) (2005).
[21] For a recent review see, e.g. S.B. Ogale, Adv. Mater. 22 (3125) (2010), and references therein.
[22] X.Y. Cui, et al., Phys. Rev. Lett. 97 (2006) 016402.
[23] G. Kresse, J. Furthmuller, Comput. Mater. Sci. 6 (1996) 15.
[24] G. Kresse, J. Furthmuller, Phys. Rev. B 54 (1996) 11169.
[25] J.P. Perdew, K. Burke, M. Ernzerhof, Phys. Rev. Lett. 77 (1996) 3865.
[26] P.D. Borges, L.M.R. Scolfaro, H.W. Leite Alves, E.F. da Silva Jr., Theor. Chem. Acc. 126 (2010) 39.
[27] V. Srivastava, et al., Indian J. Pure Appl. Phys. 46 (2008) 397.
[28] V.L. Moruzzi, Phys. Rev. Lett. 57 (1986) 2211.